A Magnetically Suspended Large Momentum Wheel

Ajit V. Sabnis,* Joe B. Dendy,† and Frank M. Schmitt‡
Sperry Flight Systems, Phoenix, Ariz.

An 800-ft-lb-sec engineering prototype momentum wheel assembly was designed and fabricated, in which a 64-lb rotor was suspended on radial-passive, axial-active magnetic bearings and rotated at 10,000 rpm. The rationale for the selection of the magnetic bearing configuration, control concepts for the active axis, and the compensation for structural interactions are discussed. Measurements of bearing stiffness and damping, drag torque, and wheel performance are presented. Testing has confirmed that low-drag, unlubricated, wear-free operation can be attained while satisfying functional spacecraft requirements. It was determined that failure of an electronic component could be safely negotiated on the touchdown ball bearings, with a redundant electronics channel being activated to restore suspension. The structural integrity of the unit was confirmed through exposure to sinusoidal vibration and launch-level random vibration. In terms of weight and power dissipation, magnetically suspended momentum wheels compare favorably with conventional wheels, and considerable weight saving may be realized if a "no single point failure" requirement exists. It is concluded that magnetic bearings are capable of providing reliable, long-life operation in momentum wheels and other spacecraft applications.

Introduction

THE use of magnetic bearings for rotational applications in spacecraft is becoming increasingly attractive, especially with the trend towards longer mission lifetimes and the emphasis on lower induced vibration. The primary advantages of magnetic bearings are low-drag torque and unlubricated, wear-free, vacuum-compatible operation. In addition, when a "no single point failure" requirement exists, benefits in the areas of power consumption and weight become possible, since redundancy can be provided by a mere duplication of the bearing control electronics.

Unlike ball bearings, magnetic bearings are an intimate part of the overall design, and cannot be specified in terms of simple mechanical interfaces. For instance, their weight is a strong function of required stiffness; furthermore, there are several bearing types, each of which can be configured in several ways. Because of this variability, many new concepts of equipment design are evolving. The problem that now exists is to develop effective designs in terms of weight, power and cost which meet specific application requirements.

The objectives of this paper are to discuss the application of magnetic bearings to large momentum wheels and, in particular, to describe the design, development, and test results on a large magnetically suspended prototype momentum wheel (nominal momentum = 800 ft-lb-sec). A review of some of the earlier work related to the development of magnetically suspended momentum wheels may be found in the paper by Henrikson et al.,[1] and the development of a 62 ft-lb-sec momentum wheel with radial-active bearings was described by Veillette.[2]

Magnetic Bearing Selection

The achievement of entirely contactless suspension is subject to the fundamental restriction of Earnshaw's theorem,[3] which specifies sufficient conditions for instability in inverse-square force fields. The practical consequence of the theorem is that stability under magnetostatic fields is impossible unless diamagnetic or superconducting materials are used. If ferromagnetic materials are used, there is at least one statically unstable coordinate direction, and suitable time-varying fields must be generated to achieve 3-dimensional stability of suspension. The term "passive" is used to describe an axis of the suspension which is magnetostatically stable, while "active" is used for an axis stabilized by dynamic fields.

Of the all-passive systems, diamagnetic bearings have inherently low specific load capacity, while superconducting bearings require the added weight and complexity of a cryogenic cooling system. Among the active systems, a.c. systems (eddy-current repulsion systems, as well as a.c. resonant systems) are characterized by heavy power loss and poor damping. For application to large momentum wheels it is therefore possible to narrow the choice to a d.c. magnetic system, in which a combination of permanent magnets and electromagnets is employed.

Rotational d.c. magnetic bearings may be divided into three classes: a) Radial-passive, axial-active; b) Axial-passive, radial-active; c) All-active.

The radial-passive, axial-active bearing needs active control of only 1 degree of freedom, and is thus capable of higher reliability. Angular stiffness may be realized passively by the provision of sufficient axial spacing between two radial-passive bearings. Its limitation is that the radial stiffness, obtained passively, is lower than the other systems of a similar size. For momentum wheel applications where high angular stiffness is not a requirement, this is not a stringent limitation. The radial passive, axial active system was therefore selected for the design. Further, the radial passive forces may be obtained through attraction or repulsion. The attraction system was chosen because: a) The flux is confined to the magnetic bearing, eliminating interactions with other components; b) The permanent magnet can be nonrotating, thus not limiting rotational speeds; c) Modulation of the bias permanent magnet field is an elegant way of generating bi-directional axial control forces. The bias field provides a high-gain, linear, control force-current characteristic.

The Three-Loop Bearing Design

A schematic of the selected design configuration is shown in Fig. 1. It has been termed a 3-loop bearing because 3 independent loop equations are required to analyze the magnetic circuit.

The bias magnetic flux (B_0) is provided by the axially magnetized ring magnet across four axial gaps, with the

Presented as Paper 74-899 at the AIAA Mechanics and Control of Flight Conference, Anaheim, California, August 5-9, 1974; submitted August 26, 1974; revision received February 13, 1975. The authors would like to thank TRW Systems, Inc. for their participation in this development.

Index category: Spacecraft Attitude Dynamics and Control.

*Principal Engineer. Member AIAA.

†Staff Engineer.

‡Senior Project Engineer.

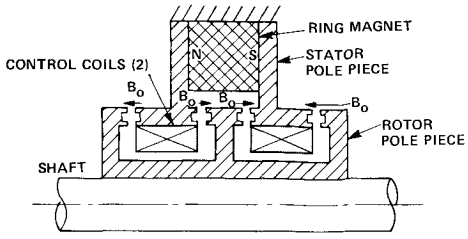

Fig. 1 Three-loop bearing, half section.

direction of the bias flux shown by the arrows in the figure. The passive radial stiffness is provided through the action (minimum reluctance) of opposed concentric rings at the air gaps, the total stiffness being proportional to the number of rings. Radial damping is improved by conducting material (copper wire) placed in the inter-ring grooves at the air gaps.

In the axial direction, the bias fields cause instability. Axial control forces are provided by modulating the gap bias fluxes. This is accomplished by varying the magnitude and direction of the current to the two control coils in response to axial position and rate. Thus, the coils are connected so that the bias flux is increased in one pair of gaps by an amount ΔB while it is decreased in the other pair of gaps. The result is an axial force proportional to $B_0 \Delta B$.

The configuration selected is similar to one developed by Studer,[1] in that a 3-loop magnetic circuit is used. However, the arrangement is different in that one permanent magnet, and 2 control coils are employed, with modulation of the bias field in all 4 axial gaps. The Studer configuration employs two magnets and one coil, which permits modulation in only 2 of the 4 gaps.

The significant features of the 3-loop configuration can be summarized as follows: a) Both magnets and coils are stationary; b) The coil current must primarily overcome only the air-gap reluctance; c) The bias field permits higher gains at lower power levels; d) Radial damping is provided by copper rings; e) Pole pieces are used to minimize flux variations at the gaps during rotation.

Design Considerations

The primary function of this momentum wheel assembly (MWA) was to serve as a test bed for the magnetic suspension system and to demonstrate the special features that are unique to a magnetic bearing MWA (MBMWA). Consequently, no major effort was made to minimize weight or size, and no specific environmental requirements were included in the design. The objective was to obtain a representative functional unit which could be tested to determine the suitability of magnetic suspension in meeting MWA performance requirements in a space vehicle. Therefore, the assembly was configured as similar to a typical MWA as possible, while using existing components (spin motor, covers, touchdown ball bearings) and incorporating features that would simplify design and fabrication.

The selection of the nominal angular momentum for the MBMWA was based on several considerations. Since the MBMWA is considered a potential replacement for a conventional 420-ft-lb-sec MWA now produced for a satellite, its parameters were used as a baseline for the sizing. This choice has the advantage of allowing a direct comparison of a magnetic bearing design with a conventional design. In addition, the approach provides a large margin for growth in momentum through increased speed, since increased momentum is anticipated for future large space vehicles. Higher operating speeds, hence lighter units, are now possible, since a magnetic bearing does not have the penalties associated with higher speeds that a ball bearing does, that is, greatly increased power dissipation and decreased life expectancy.

Accordingly, it was decided to design for an angular momentum of 400 ft-lb-sec at 5000 rpm, with a rotor radius of 20.4 in. The allowable operating speed for this rotor, as determined by rotational stresses, is 12,200 rpm, corresponding to a momentum of 1000 ft-lb-sec.

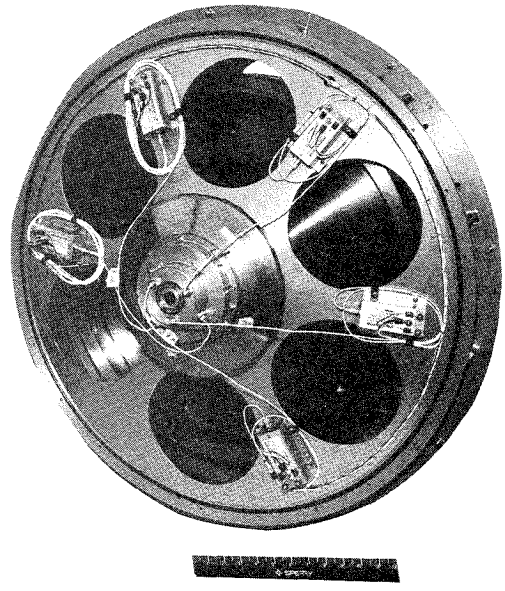

Fig. 2 Magnetic bearing momentum wheel assembly.

The size and weight of a magnetic bearing are strongly dependent on stiffness and load capacity requirements, and particular attention must be given to the choice of design stiffness values. The necessary constraints on radial stiffness were formulated, considering: a) Operating Attitude—The weight of the rotor must be supported with the spin axis horizontal or vertical, and functional requirements must be met in both 0g and 1g environments; b) Cross-Axis Rate—The specified cross-axis rate must be sustained without touchdown. A value of 3 deg/sec was chosen for the prototype design; c) *H*-Vector Misalignment—The angular stiffness must be sufficient to limit the misalignment under specified rates during operation; d) Resonance Speeds—Because of the need to minimize the radial stiffness, the wheel must operate above one or more resonances, and must therefore traverse them during run up. The resonance speeds must be adequately separated to minimize the possibility of touchdown due to residual wheel unbalance. Further, the normal operating wheel speed must be spaced sufficiently from the resonances. A factor of $\sqrt{2}$ was chosen for the design.

Having selected the radial-passive, axial-active, 3-loop configuration, its influence on the overall design must be examined. The achievement of angular stability dictates the use of two bearings with sufficient axial spacing between them. By this means angular stability is achieved passively, since the stabilizing torque of the bearing pair, due to radial restoring forces, is made to exceed the destabilizing torque due to the axial unbalance forces. A value of 3 was chosen for the ratio of axial spacing to mean ring diameter. The possibility of power failure or electronics failure with the wheel operating at high speeds presents survival and safety problems. Accordingly, the touchdown system incorporates ball bearings which, in addition to preventing contact of spin motor and magnetic bearing elements, permit the wheel to operate safely at acceptable torque levels in the event of a failure. Another influence is on the design of a motor in which the radial clearance must be larger than in conventional systems and the radial unbalance stiffness must be small in comparison to the bearing stiffness. This dictated the choice of an a.c. induction motor.

Design Description

Overall Design

A photograph of the MBMWA is shown in Fig. 2, a half-section in Fig. 3, and a weight tabulation in Table 1. The con-

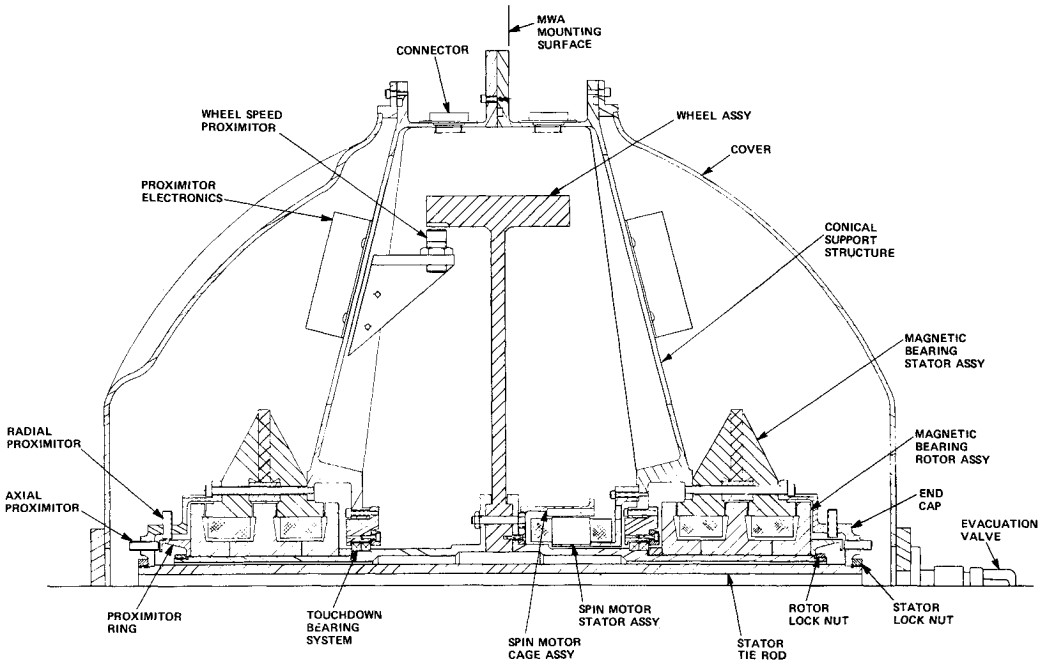

Fig. 3 Momentum wheel assembly section view.

ventional *I*-shape was selected for the rotor cross section, because is provides representative inertia, weights, and stiffness in a simple design which can be economically fabricated. For the material, 6AL-4V titanium was chosen because it is dimensionally stable, nonmagnetic, has a high elastic limit, and a high strength-to-density ratio (σ/ρ). With a given configuration, use of a material with a high σ/ρ allows higher speeds and therefore a high momentum-to-weight ratio.

The supporting structure of the MBMWA consists of two halves joined together at the center to form a mounting flange. A central tie rod, which is interior to the wheel shaft, connects the structure halves together through the end caps and magnetic bearing stators. This additional rigidity is required because the axial unbalance force of each magnetic bearing would otherwise cause excessive relative deflections of the magnetic bearing stators. Two hemispherical covers, mounted to flanges with O-ring seals, allow the entire unit to be evacuated to eliminate windage drag on the wheel. The covers are fastened to the o.d. of the structure to prevent forces on the magnetic bearing system due to the pressure differential.

A touchdown system is incorporated in the design to prevent the complete closing of the magnetic bearing air gaps and resulting damage to the rings. This system consists of ball bearings mounted on the rotor while their outer races are free to move axially and radially within the constraints of a sleeve mounted in the housing.

The touchdown ball bearings are located immediately inboard of the magnetic bearings. Thus the structural compliance between them is a minimum and does not further reduce the difference between the touchdown bearing clearance and the axial air gap of the magnetic bearings. The touchdown sleeve in the housing is sized to allow 0.008 in. axial travel in either direction, and 0.0125 in. movement in all radial directions. Mounting of the touchdown bearings on the rotor shaft rather than in the housing structure positively locates the spin axis, as determined by the touchdown bearings, near the spin axis as determined by the magnetic bearings.

Three eddy-current position sensors (proximitors) are mounted in the end cap at one end to provide axial position signals for the control system. There are also 2 radial position sensors 90° apart at each end. These 4 sensors are used to monitor radial and angular displacements of the rotor in 2 perpendicular planes through the spin axis of the rotor. The sensor electronics are mounted on the structure inside the MBMWA to minimize lead length from the sensor probes. A position sensor is also used to sense speed at the i.d. of the wheel rim. Equally spaced grooves cause four pulses per revolution for input to the speed control loop. The spin motor used is a 2-phase, 6-pole induction motor with a rotor-stator gap of 0.024 in.

Table 1 MWA weight tabulation (pounds)

Wheel assembly		64
Rotor	49.5	
Magnetic bearing rotors (2)	12.0	
Miscellaneous	2.5	
Magnetic bearing stator assemblies (2)		44
Magnets (12 segments per bearing)	3.6	
Pole pieces (4)	34.8	
Coils (4)	4.0	
Spacer ring (2)	1.8	
Housing assembly		26
Covers		24
Miscellaneous		5
Total		163

Magnetic Bearings

Following the selection of the bearing configuration and the determination of the required bearing stiffness, the next step is the design of the magnetic circuit. This involves the design of the gap geometries and magnetic structures, choice of magnetic materials, and sizing of the permanent magnet and the control coils. An important design parameter to be established is the unbalance stiffness ratio. This is the ratio of the axial unbalance stiffness to the passive radial stiffness, and is the main parameter coupling the radial and axial axes.

The stiffnesses for a concentric ring geometry are derivable by extension from a 2-dimensional analysis using conformal transformations.[4] The initial radial stiffness may be written

$$K_r = \alpha n r (B_g)^2 \tag{1}$$

where α = a coefficient dependent on geometry, n = the number of concentric rings, r = the mean radius at the rings, B_g = the peak flux density in the gap.

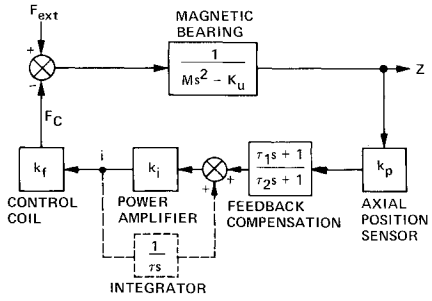

Fig. 4 Axial control system.

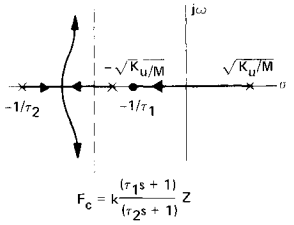

Fig. 5 Root locus, lead compensation.

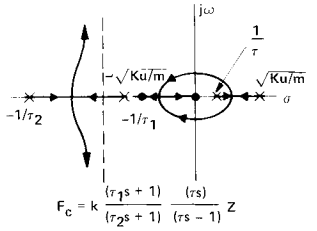

Fig. 6 Root locus, integral feedback.

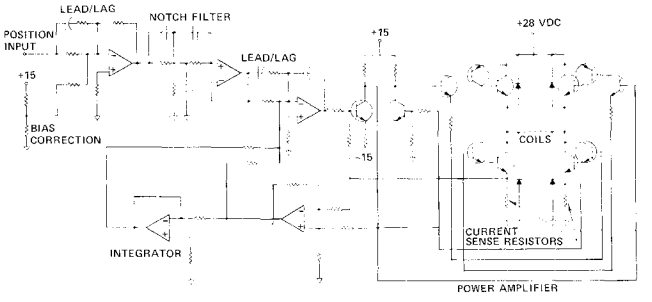

Fig. 7 Control electronics simplified schematic diagram.

The design value of radial stiffness, chosen on the basis of the stiffness constraints, was 5000 lb/in. per bearing, and a gap flux density $B_g = 0.8$ Wb/m^2 was chosen, allowing a modulation margin before saturation. For a mean radius of 2 in. at the rings, the number of rings per gap was determined to be 8. Samarium-cobalt was selected as the permanent magnet material because of its high energy product, low recoil permeability, high intrinsic coercive force, and its reversible demagnetization characteristic. To minimize the unbalance stiffness ratio, a ring land thickness of 0.014 in. was chosen, being a practical minimum from machining and strength considerations. The axial gap was selected as 0.015 in., and the groove width between rings 0.035 in., a value where there would be little interaction between adjacent rings. The design of the radial system was completed by sizing the permanent magnet for the design B_g and gap geometry.

The expected value of unbalance stiffness ratio was calculated to be -7.9 and the required coil ampere-turns to be 1040. The pole-pieces and the control coils were sized suitably, with a titanium spacer ring used to separate and align the stator pole-pieces. The spacer also prevented clamping and reaction forces being applied to the magnets. The permanent magnet was an annular ring, made from 26 separate segments, and insertion into the bearing was accomplished after assembly of all the other parts. Thus, the large axial unbalance force normally present does not pose assembly problems.

Control Concepts for the Active Axis

As a consequence of Earnshaw's theorem, the radial restoring stiffness of the passive magnetics is accompanied by instability in the axial direction. The unbalance force in the axial direction is a linear function of axial displacement near the equilibrium position. The axial equation of motion of the magnetic suspension is therefore given by

$$M\ddot{z} - K_u z = F \tag{2}$$

where z = axial displacement from the equilibrium position, M = suspended mass, K_u = unbalance stiffness, F = applied force (total).

Axial stability can be obtained by controlling the current to the control coils to generate forces in the proper direction. Thus, if the control force includes rate-plus-displacement feedback given by

$$F_c = -B\dot{z} - Kz, \tag{3}$$

then the axial equation of motion becomes

$$M\ddot{z} + B\dot{z} + (K - K_u)z = F_{ext} \tag{4}$$

where F_{ext} is the external force. This equation indicates system stability can be obtained for $B > 0$, $K > K_u$, a net static stiffness of $(K - K_u)$ and resultant power loss under external axial loads. In practice, the rate sensor may be avoided by using lead compensation of the position signal. A block diagram of the axial control system is shown in Fig. 4, and the root locus in Fig. 5.

In addition to the lead compensation, a minor loop integrator can be added (shown by dashed lines in Fig. 4), in order that the unbalance stiffness of the passive magnetics can be used to advantage in overcoming external loads. The integrator enables zero power dissipation in the coils under steady axial loads. The integrator also enables long-term, low-power operation by correcting for drift in any of the electronic components, including the position sensor. With integral feedback, the static axial stiffness is negative, $-K_u$; the root locus of this system is shown in Fig. 6. It may be noted that the action of the minor loop integrator is similar to that of the "virtually zero power" system,[1] both methods providing a right-half plane pole and a zero at the origin. However, the virtually zero power system necessitates a velocity sensor, and cannot independently achieve suspension, being velocity-based; suspension is achieved through the initial use of a position-sensor.

Electronics

The suspension electronics consists of a position sensor, compensation networks, and a current amplifier for driving the coils in the magnetic bearing. A schematic diagram is shown in Fig. 7.

The axial position sensor used is an eddy-current sensor having an output which varies from about 0-15 v d.c. over a range of 0-0.050 in. It is adjusted to provide an output of -8 v d.c. when the wheel is levitated, and no external forces are applied.

In the electronics, a $+8$ v d.c. signal is introduced to correct for this offset. Any difference between the sensor output and the $+8$ v d.c. bias correction signal results in steady-state coil currents and a corresponding power loss. Therefore, an integrator is used with the single channel electronics to automatically adjust this bias correction to maintain zero

steady-state coil current. It not only corrects for sensor installation and bias errors, but also reduces steady-state coil current to zero in the presence of external forces, such as gravity, on the rotor. The integrator moves the position reference command so that the unbalance force of the passive magnetics just balances the external force, and no additional force provided by coil currents is needed.

As previously discussed, based on linear rigid body analysis, the only compensation necessary would be a single lead/lag network to overcome the axial static unbalance. However, there were structural resonances that required additional compensation. A second lead/lag network and a notch filter satisfied the requirements very well. The structural resonances and compensation, along with measured frequency responses, are discussed in the test results.

A linear power amplifier design was decided upon as opposed to a switching amplifier using pulsewidth modulation. The linear amplifier is simpler; also, the expected power required to maintain suspension is small, thus not justifying a switching amplifier.

The magnetic bearing coils, driven by the amplifier, may be connected in several configurations, that is, series, parallel, or series-parallel. It takes 2.5 amp per coil to levitate, so if a series connection of the coils is used only a small amplifier is needed. However, in anticipation of a possible problem because of current rate limit caused by the coil inductance, it was decided to make the amplifier capable of driving the four coils in parallel (10 amp). Hence, an amplifier able to deliver up to 15 amp was developed. The frequency characteristic of the amplifier is that of a first-order lag having a 3 db bandwidth of about 4 KHz.

It was initially planned to use redundancy in the control electronics because of the unknown safety risk and possible damage to the MWA in case of an accidental touchdown at high speed. However, it was found during the initial testing that touchdowns could be safely negotiated at speeds up to 10,000 rpm without any adverse effects. Consequently, although preliminary testing of the redundant system was carried out successfully, further development was deferred until other MWA tests were completed.

Test Results

A summary of the principal results to date is shown in Table 2.

Table 2 MBMWA Test results summary

Polar inertia (total)	0.78 ft-lb-sec^2
Maximum momentum achieved (10,000 rpm)	800 ft-lb-sec
Cross-axis rate capability at 400 ft-lb-sec	2.8 deg/sec
Wheel balance	
static	<0.02 oz-in.
dynamic	<0.25 oz-in.^{2}
Critical speeds	
radial	2380 rpm
angular	7800 rpm
Drag torque coefficient (two bearings)	0.08 oz-in./ 1000 rpm

Magnetic Bearings

All the tests were conducted with 12 magnet segments per bearing. Insertion of more segments showed only small increases in the radial stiffness, possibly an indication that saturation of the iron was being approached. The gap flux density was measured at 0.72 Wb/m^2 using a Hall-probe gaussmeter. This measurement was made with the smallest probe presently available, but is an average measurement because the probe dimensions exceed the ring land width in the geometry. Leakage flux density measurements revealed that the leakage was lower than estimated; reductions in bearing weight for subsequent designs therefore appear possible.

The radial force-displacement characteristics are shown in Fig. 8. The stiffness characteristic of both bearings was substantially the same, having a slope of 3640 lb/in. at zero deflection. The general shape of the curves is as expected for the geometry, showing good linearity to a displacement of about $0.6T$ (ring land width) $= 0.008$ in.

The total unbalance stiffness in the axial direction was measured as the static stiffness with the integral feedback loop in operation. The measured stiffness was $-44{,}000$ lb/in.

The angular stiffness was measured by applying point loads to the rim, and then again by applying pure moment loads on the rim; the spin axis was vertical in each case. The results are plotted in Fig. 9, with the deflection angle computed from the radial proximitor readings. Both methods show good

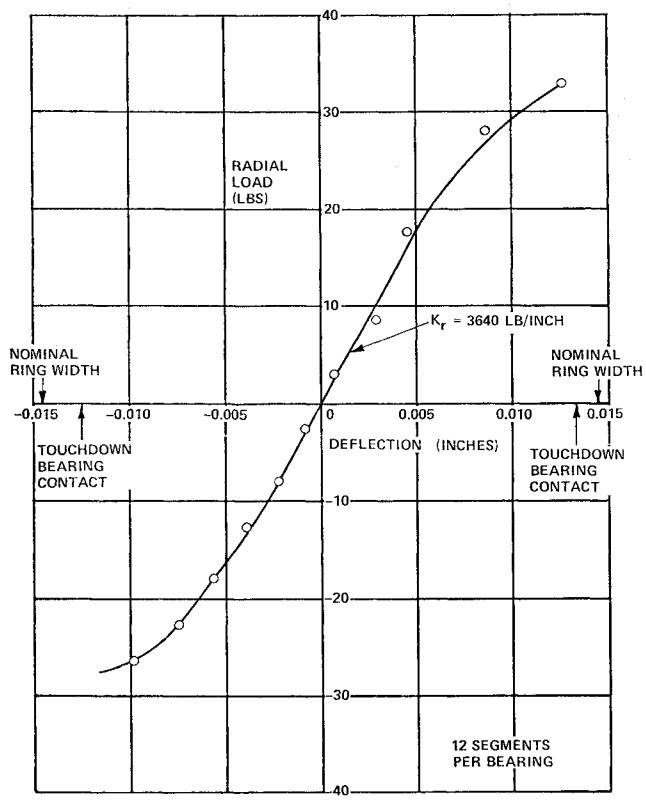

Fig. 8 Measured radial stiffness of one bearing.

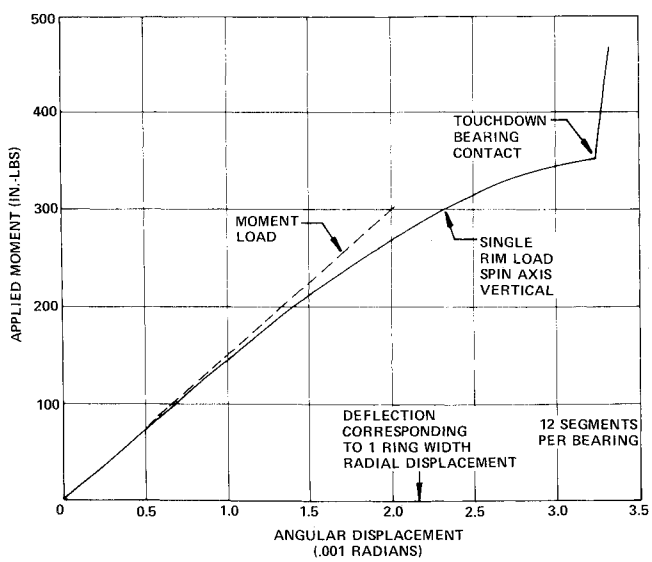

Fig. 9 Magnetic bearing momentum wheel assembly angular stiffness.

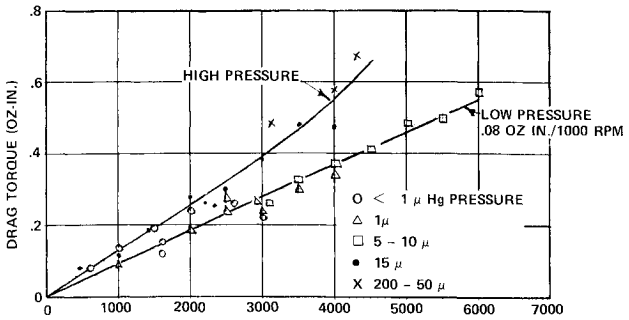

Fig. 10 Drag torque, momentum wheel assembly.

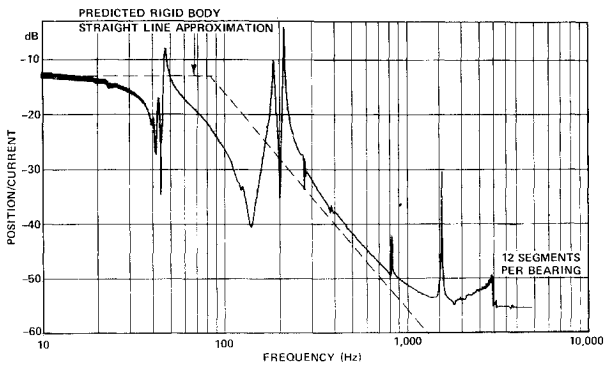

Fig. 11 Magnetic bearing transfer function, gain.

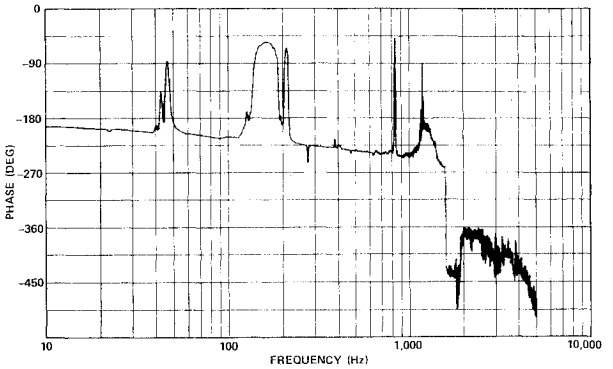

Fig. 12 Magnetic bearing transfer function, phase.

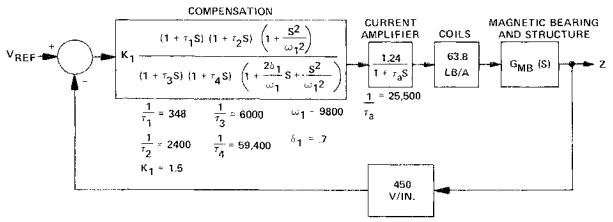

Fig. 13 Axial control system.

agreement at the origin, but the stiffness measured by a single point load decreases at higher deflection angles. This is attributed to the effects of radial and axial displacement inherent in this test method.

The radial damping was measured by recording the radial proximitor outputs in response to a radial impulse force. The damping coefficient for nominal radial displacement (± 0.0005 in.) was calculated to be 0.37 lb/in./sec per bearing. This was a factor of 3 greater than the coefficient previously measured without any conductive rings. In this case, copper rings had been cemented in between the rings in the stators (only) of the bearing. This increase in damping coefficient is desirable from the viewpoint of rotor-dynamics, and confirmed that the provision of conductive material in the inter-ring grooves does lead to an increase in the damping by providing extra eddy-current losses. The test was repeated at larger displacements and smaller displacements, and the coefficients were found to be 0.6 and 0.16 lb/in./sec, respectively. Thus, the damping was observed to be a function of displacement. The larger deflections were ~ 0.0015 in.; the smaller displacements ~ 0.0001 in.

Drag torque data was taken on both a test rotor assembly (20 lb, 8 in. diam), and the large MWA wheel (64 lb). The test rotor was used to minimize the effects of loads and windage, and thereby obtain the torque attributable only to the bearings. One additional difference was that copper wires (to obtain radial damping) were present in the magnetic bearing stators during the MWA tests, whereas they were absent in the test rotor measurements. All test data was taken by measuring coast-down times. Also, the tests were conducted with the spin axis vertical, after it was determined that the wheel attitude did not significantly affect the torque data.

The bearing drag with the test rotor was quite low, having a slope of 0.03 oz-in. per 1000 rpm. This speed-dependent torque is due to eddy currents, and can be extended linearly to higher speeds. Figure 10 shows the torque data taken at various housing pressures for the MWA. Two torque curves are illustrated, one through the various data points for high pressures ($>20\ \mu$), and one for low pressure ($<10\mu$). The data was placed into these two categories on the basis of observed grouping. The MWA wheel has greater sensitivity to the ambient pressure than the test rotor because of its larger radius, and thus lower pressures were necessary before the drag torque showed no further decrease. At low pressure, the windage can be assumed negligible.

The slope of the line through the low pressure points is 0.08 oz-in. per 1000 rpm, and is considered to represent the bearing system torque as installed in the MWA. It is substantially linear with speed, but shows an increase over the 0.03 value measured on the test rotor. This difference may be attributable to additional eddy current losses in the copper rings placed in the magnetic bearing stators in the MWA. These rings have been shown to increase the damping of radial motion by a factor of 3, and they could also cause drag torques by a similar mechanism, but in a rotational sense.

Control System and Electronics

Power consumption

The power consumption of the suspension electronics was approximately 3 w at zero speed and increased to 5 w at a speed of 1000 rpm. Power consumption was relatively independent of speed between 1000 and 5000 rpm, except for a sharp peak up to 12 w at 2380 rpm, the location of the rotor radial resonance.

The reason power loss increases at operating speeds is that rotational frequency signals are picked up by the axial position sensor. Because of the need for the tie rod, the sensor cannot be placed at the center of the shaft, but is offset to one side. Hence, any angular motion of the rotor or mechanical runout of the sensed surface is picked up by the sensor. These effects were minimized by placing three sensors at 120° intervals around the shaft and averaging their outputs.

Control loop dynamics

The open-loop transfer function for the magnetic bearing is nonminimum phase (one right half-plane pole); the stability criterion is therefore that the Nyquist locus must encircle the -1 point once. The stabilization of the control loop is complicated by the presence of numerous resonances of the momentum wheel and its mounting structure. Figures 11 and 12 show the gain and phase responses of the magnetic bearing and supporting structure. Stabilization requires shifting the phase curve up above $-180°$ out to the frequency where the loop gain drops below 0 db. The block diagram of the control system is shown in Fig. 13. The lowest frequency structural

mode at about 50 Hz was caused by the supporting structure base plate. It had no adverse effect on bearing operation. Because of the high gain at 210 Hz, it is difficult to gain stabilize the loop, and maintain adequate phase lead at lower frequencies. Phase stabilization was therefore used to provide lead at frequencies up to 270 Hz.

There was a special problem at 270 Hz because the phase characteristic there lags by 30° in a manner caused by a complex pair of poles and a nearby complex pair of zeros at a slightly higher frequency. This is peculiar in that in all other cases of structural resonance the complex pair of zeros occurs at a lower frequency than the poles, giving rise to a leading phase shift. Analysis shows that this situation can result from compliance between the two bearings at opposite ends of the shaft. This was confirmed by operating the wheel with only one bearing and measuring the frequency response. The phase shift was then leading instead of lagging at that resonance. Stable support was obtained when operating with only one bearing.

In addition to the phase peaks and dips at the structural resonances, it can be seen that there is also a gradual phase lag, corresponding to a pole at about 260 Hz. This gradual lag is due to hysteresis and eddy-current losses. In essence, these losses cause a phase lag between the coil current and the control force.

The phase stabilization of the bearing thus required the addition of 75° of phase lead at 270 Hz. A dual lead/lag network was used to provide the required phase lead. This increased the gain at high frequencies to such an extent that the rotor web resonance at 1580 Hz became unstable. A notch filter was used at that frequency.

One problem with the control system was a nonlinear oscillation which could start when a severe disturbance, either mechanical or electrical, was applied to the bearing. The rotor would oscillate back and forth, hitting the touchdown bearings with an accompanying loud noise. It is apparently a complex interaction between the flexible housing, the mechanical stops, amplifier saturation, and gain and phase characteristics of the loop. To eliminate this problem completely it is necessary to gain stabilize rather than phase stabilize the housing mode. This can be done most easily by modifying the mounting structure and housing stiffness to reduce the resonant peaks and increase the resonant frequency. Then gain stabilization with a second-order, low-pass filter would be possible.

An approach to redundancy that appears very promising for spaceflight applications is possible, since operation of the MWA with only one bearing provides such good performance. A dual-redundant system is suggested whereby one channel is connected to each bearing and used on an operate-standby basis. When a failure of one channel occurs, as detected by touchdown of the rotor, the second channel would be activated. In cases where it is undesirable to have rotation on touchdown bearings for any significant period, the detection and switching could be made automatic.

Rotor Dynamics and Cross-Axis Rates

There are several unconventional features of the MBMWA design which could potentially affect the dynamics during a run-up to operating speed, and also the behavior of the unit when subjected to a cross-axis rate. First, the suspension system is much more compliant than a comparable ball-bearing system, and the damping is relatively light. The suspension system has touchdown bearings which come into play at extreme displacements. Also, the rotor is really not a rigid body but rather three masses, the rim, and two magnetic bearing rotors. These masses are connected by the web and the shafts, which are fairly compliant.

A preliminary analysis was performed to determine the critical speeds and to confirm that reasonable displacements would be encountered when passing through criticals with reasonable rotor balance levels. The analysis predicted critical speeds of 1900 and 7600 rpm. MWA tests showed good agreement, with the radial resonance at 2380 rpm and the angular resonance at 7800 rpm.

During the initial run up of the rotor, the axial control system was intentionally deactivated at many different speeds. The purpose of this was to determine if the rotor could shift from the spin axis defined by the magnetic bearings to that defined by the touchdown bearings in a stable fashion. It was found that this transition was well-behaved. Orbits of the ends of the shaft were monitored during touchdown, and no significant changes were observed. The touchdown speed ranged from 0-10,000 rpm.

Testing was performed to verify that the MBMWA was able to sustain cross-axis rates in a stable and predictable manner. The measurements were limited to wheel speeds of 5000 rpm (400 ft-lb-sec) and cross-axis rates of 3.5° per sec because the wheel had not been completely overspeed tested at the time of these tests. The gyroscopic torque causes deflections of the rotor which were monitored with the radial proximitors.

These tests verified that the response of a magnetically suspended rotor to a dynamically applied transverse torque is virtually identical to its response to a statically applied torque. The unit was also subjected to cross-axis rates sufficient to cause radial contact at speeds up to 5000 rpm; the touchdown was found to be well behaved.

Vibration Testing

Because of the unique and untested mechanical features, and in anticipation of the launch vibration environment a flight magnetic bearing momentum wheel would have to survive, the MBMWA was subjected to sinusoidal and random vibration. A series of ½g sinusoidal tests were conducted to determine the general dynamic characteristics of the unit with the rotor nonlevitated, such as resonant frequencies, transmissibilities and mode shapes. Based on the sinusoidal test results, it was determined, analytically, that the MBMWA could survive a launch-level random vibration. The random vibration test input levels were 12g rms axially, and 11g rms radially. Post-vibration testing of the unit showed no functional, magnetic, or dimensional changes. Disassembly and inspection of the touchdown and magnetic bearing parts showed no evidence of damage.

Conclusions

The experience gained during the construction and test of the engineering prototype momentum wheel assembly indicates that magnetic suspension is applicable to large momentum wheels without an appreciable effect on weight and power. In fact, the specific 3-loop bearing system and MWA design concepts developed during this program can be effectively employed over the same range of momentum wheel sizes which are conventionally supported by ball bearings. Additionally, the magnetic bearing design provides the capability for reliable, low-drag torque operation over a much greater speed range than ball bearings, extending from stall to speeds that are limited only by stress considerations of the rotating parts.

The concept of total spin-bearing redundancy within a single mechanical structure was proven to be feasible. Thus, a weight reduction approaching 2:1 is possible when compared with a spacecraft system which requires a second MWA to avoid single point failures. Since the coils in each magnetic bearing are independently capable of controlling the axial system, a natural redundancy scheme is possible by using two position sensors and two channels of electronics. A failure is simply detected at the position sensor, which causes spacecraft power to be removed from the failed channel and applied to the standby channel. The use of this standby redundancy technique is possible because of the successful performance of the ball-bearing touchdown system.

The most significant design parameter to consider for an MBMWA is the radial stiffness (k_r) of the magnetic bearing.

There are constraints on k_r that exist within the MWA design itself, such as separation of natural frequencies from each other and from wheel speed. Also, if the requirement exists to operate in a 1g environment with the spin axis horizontal, it is probable that this will establish the minimum value of k_r. The most significant constraint remaining is the minimum angular stiffness of the rotor support system, which is influenced mainly by k_r of the bearings. Thus, it is of primary importance to specify the minimum acceptable value of angular stiffness to achieve the lowest possible bearing system weight.

Design improvements are possible to reduce overall weight and improve the general structural design. It is estimated that a 1200-ft-lb-sec wheel would weigh 115 lbs and operate at 10,000 rpm.

The MWA would need to be optimized to determine wheel speed and diameter, based on weight and power considerations. Because of the scope of the present program, no optimization was performed. Because of the low drag torque of magnetic bearings, it is likely that the optimal speeds will approach stress-limited speeds for the material of the rotor.

Testing and evaluation of the present MBMWA revealed no major shortcomings of the design. The design, as it now stands, could serve as the basis for a prototype flight design.

References

[1] Henrikson, C.H., Lyman, J., and Studer, P.A., "Magnetically Suspended Momentum Wheels for Spacecraft Stabilization," AIAA Paper 74-124, Washington, D.C., 1974.

[2] Veillette, L.J., "Design and Development of a Momentum Wheel with Magnetic Bearings," *Proceedings of the 8th Aerospace Mechanisms Symposium,* sponsored by NASA, Lockheed Missiles and Space Co., Inc. and California Institute of Technology, Hampton, Va., Oct. 1973.

[3] Earnshaw, S., "On the Nature of Molecular Forces," *Transactions of the Cambridge Philosophical Society,* Vol. 7, 1842, pp. 97-112.

[4] Sabnis, A.V., "Analytical Techniques for Magnetic Bearings," Ph.D. dissertation, May 1974, Dept. of Mechanical Engineering, University of California, Berkeley, Calif.